Reactions of Dimethylsulfoxide Reductase in the Presence of Dimethyl Sulfide and the Structure of the Dimethyl Sulfide-Modified Enzyme[†,‡]

Robert C. Bray,*[,§] Benjamin Adams,[||] Andrew T. Smith,[||] Raymond L. Richards,[§] David J. Lowe,[⊥] and Susan Bailey[#,▼]

School of Chemistry, Physics, and Environmental Science, University of Sussex, Brighton, BN1 9QJ, U.K., School of Biological Sciences, University of Sussex, Brighton, BN1 9QG, U.K., John Innes Centre, Norwich, NR4 7UH, U.K., and CLRC Daresbury Laboratory, Warrington, WA4 4AD, U.K.

Received March 19, 2001; Revised Manuscript Received June 7, 2001

ABSTRACT: The bis-molybdopterin enzyme dimethylsulfoxide reductase (DMSOR) from *Rhodobacter capsulatus* catalyzes the conversion of dimethyl sulfoxide (DMSO) to dimethyl sulfide (DMS), reversibly, in the presence of suitable e^--donors or e^--acceptors. The catalytically significant intermediate formed by reaction of DMSOR with DMS ('the DMS species') and a damaged enzyme form derived by reaction of the latter with O_2 (DMS-modified enzyme, $DMSOR_{mod}D$) have been investigated. Evidence is presented that Mo in the DMS species is not, as widely assumed, Mo(IV). Formation of the DMS species is reversed on removing DMS or by addition of an excess of DMSO. Equilibrium constants for the competing reactions of DMS and DMSO with the oxidized enzyme ($K_d = 0.07 \pm 0.01$ and 21 ± 5 mM, respectively) that control these processes indicate formation of the DMS species occurs at a redox potential that is 80 mV higher than that required, according to the literature, for reduction of Mo(VI) to Mo(IV) in the free enzyme. Specificity studies show that with dimethyl selenide, DMSOR yields a species analogous to the DMS species but with the 550 nm peak blue-shifted by 27 nm. It is concluded from published redox potential data that this band is due to metal-to-ligand charge transfer from Mo(V) to the chalcogenide. Since the DMS species gives no EPR signal in the normal or parallel mode, a free radical is presumed to be in close proximity to the metal, most likely on the S. The species is thus formulated as $Mo^V-O-S^{\bullet}Me_2$. Existing X-ray crystallographic and Raman data are consistent with this structure. Furthermore, $1e^-$ oxidation of the DMS species with phenazine ethosulfate yields a Mo(V) form without an −OH ligand, since its EPR signal shows no proton splittings. This form presumably arises via dissociation of DMSO. The structure of $DMSOR_{mod}D$ has been determined by X-ray crystallography. All four thiolate ligands and Oγ of serine-147 remain coordinated to Mo, but there are no terminal oxygen ligands and Mo is Mo(VI). Thus, it is a dead-end species, neither oxo group acceptance nor e^--donation being possible. O_2-dependent formation of $DMSOR_{mod}D$ represents noncatalytic breakdown of the DMS species by a pathway alternative to that in turnover, with oxidation to Mo(VI) presumably preceding product release. Steps in the forward and backward catalytic cycles are discussed in relation to earlier stopped-flow data. The finding that in the back-assay the Mo(IV) state may at least in part be by-passed via two successive $1e^-$ reactions of the DMS species with the e^--acceptor, may have implications in relation to the existence of separate molybdopterin enzymes catalyzing DMSO reduction and DMS oxidation, respectively.

Periplasmic dimethylsulfoxide reductase (DMSOR)[1] from the photosynthetic bacteria *Rhodobacter capsulatus* and *Rhodobacter sphaeroides* (*1*, *2*) is a bis-molybdopterin enzyme. Very closely related are trimethylamine *N*-oxide reductase from *Shewanella massilia* (*3*) and biotin sulfoxide reductase from *Rhodobacter sphaeroides* (*4*). DMSOR is regarded as a key member of the large family of enzymes

[†] Work at Daresbury Laboratory was supported by BBSRC Grant B08009 and that at University of Sussex in part by a grant from the Wellcome Trust.

[‡] The atomic coordinates and observed structure factors for the new dimethylsulfoxide reductase structure have been deposited in the Protein Data Bank under file name 1h5n.

* To whom correspondence should be addressed at the School of Chemistry, Physics, and Environmental Science, University of Sussex, Brighton, BN1 9QJ, U.K. Telephone: +44-1273-678135, FAX: +44-1273-677196, E-mail: r.c.bray@sussex.ac.uk.

[§] School of Chemistry, Physics, and Environmental Science, University of Sussex.

[||] School of Biological Sciences, University of Sussex.

[⊥] John Innes Centre.

[#] CLRC Daresbury Laboratory.

[▼] Present address: Lawrence Berkeley National Laboratory, Berkeley, CA 94720.

[1] Abbreviations: DMS, dimethyl sulfide; DMSO, dimethyl sulfoxide; DMSe, dimethyl selenide; DMSeO, dimethyl selenoxide; DMSOR, dimethylsulfoxide reductase. Variants of the enzyme: $DMSOR_{ap}$, oxidized enzyme as purified by standard procedures; $DMSOR_{rc}$, enzyme submitted to a cycle of reduction and reoxidation ('redox-cycling'), using prescribed procedures; $DMSOR_{mod}D$ [originally $DMSOR_{mod}$ (*23*)], modified form prepared by extended aerobic exposure to DMS; $DMSOR_{mod}H$, modified form obtained specifically on aerobic exposure to Na^+-Hepes. Other abbreviations: PEG, poly(ethylene glycol); rmsd, root-mean-square deviation from ideality; MPT, molybdopterin; MGD, molybdopterin guanine dinucleotide; PES, phenazine ethosulfate; DCPIP, 2,6-dichlorophenolindophenol; MV, methyl viologen; $MV^{\bullet}$, methyl viologen radical; BV, benzyl viologen; $BV^{\bullet}$, benzyl viologen radical; TMA, trimethylamine; TMAO, trimethylamine *N*-oxide; LMCT, ligand-to-metal charge transfer; MLCT, metal-to-ligand charge transfer.

10.1021/bi010559r CCC: $20.00
Published on Web 07/19/2001

(*5*, *6*) that includes formate dehydrogenases and respiratory nitrate reductases. DMSOR catalyzes the final step of a respiratory chain with DMSO as the terminal electron acceptor:

$$DMSO + 2e^- + 2H^+ \leftrightarrow DMS + H_2O$$

This reaction is of environmental significance in a variety of contexts (*7*−*10*), perhaps most notably in relation to the established role (*8*) of DMS in cloud formation. Unusually among molybdenum enzymes (*5*), DMSOR contains molybdopterin as its sole cofactor, lacking heme, flavin, and iron−sulfur centers. Because of its relatively ready availability and simplicity of structure, it should be the most accessible and, hence from a mechanistic point of view, the most definitive member of this important family. For this reason, it has been extensively studied not only by X-ray crystallography (*3*, *11*−*17*), but also spectroscopically, e.g., by EPR (*1*, *18*, *19*), EXAFS (*19*, *20*), and Raman spectroscopy (*4*, *21*, *22*), as well as by UV/visible spectroscopy, including fast kinetic studies (*15*, *23*). Nevertheless, until very recently, there remained much controversy concerning the structure of the active center of the enzyme and hence its reaction mechanism. This has now largely been resolved (*15*, *16*), following the finding (*15*) that, under certain conditions, DMSOR is susceptible to specific damage by molecular oxygen. This involves conversion to the modified form, $DMSOR_{mod}H$, in which dissociation from the metal has occurred, of both thiolate ligands of one MGD molecule. Since the enzyme is produced only by organisms growing anaerobically but is isolated and handled aerobically, it is not surprising that oxygen should have such harmful effects. That these had earlier remained unsuspected is due to their ready reversal under the conditions of the standard forward assay. The thiolate-dissociated enzyme is, however, inactive in the alternative backward assay (*23*). The use of the latter thus facilitated detection (*15*) of this damaged form. Conditions analogous to those in the forward assay, i.e., reduction by $MV^{\bullet}$ followed by reoxidation by DMSO, can be used to 'redox-cycle' the protein, a treatment used (*15*) for preparing homogeneous enzyme that is particularly important when recombinant enzyme is employed (*24*). It is now agreed (*15*, *16*) that in the structure of the undamaged physiologically active oxidized enzyme, all four thiolates from the MGD cofactors are coordinated to the metal, as is the hydroxyl group of serine-147. There is also an oxo ligand [O2, in the nomenclature of ref (*11*) and oxo1 in ref (*16*)] at the position in the structure taken up by a bound DMSO molecule (*11*). This oxygen is undoubtedly the atom shown (*21*) by Raman spectroscopy to be transferred in catalysis. The other oxygen [O1 of ref (*11*)], detected in all the early structures, will not be further considered here, as it may be an artifact (*15*, *16*). That such an artifact could arise stems from the likelihood that all enzyme crystals studied to date have been mixtures in different proportions of the fully coordinated active enzyme and the thiolate-dissociated inactive form, with the electron-dense molybdenum atom of the latter coinciding in the structure with the position of O1 of the former.

Brief reaction of the enzyme with DMS leads to a marked alteration in its UV/visible spectrum; this changes from a form with $\lambda_{max} = 720$ nm and shoulders at 560 and 470 nm, to one with $\lambda_{max} = \sim 550$ and ~ 480 nm (*11*). Stopped-flow kinetic studies have shown (*23*) that this reaction takes place at a catalytically competent rate. The present work arose because features of this reaction seemed inconsistent with the generally accepted conclusion (*11*, *19*−*21*) that molybdenum in the product is Mo(IV). In work seeking further to exploit the unique potential of UV/visible spectroscopic studies of DMSOR, we have reinvestigated the nature of this enzyme intermediate (termed here 'the DMS species', rather than 'DMS-reduced enzyme' or 'DMSOR in complex with DMSO'). Spectroscopic and equilibrium studies led us provisionally to formulate the species as $Mo^{V}-O-S^{\bullet}Me_2$. This proved consistent with other data, including the crystallographic structure which we now report, of $DMSOR_{mod}D$, an oxygen-damaged form studied earlier (*23*). The work provides new insights into the relationship between the forward and backward enzyme-catalyzed reactions of DMSOR.

MATERIALS AND METHODS

DMSOR Samples and Activity Assays. The enzyme was isolated from *Rhodobacter capsulatus* as described by Bray et al. (*15*) and was subjected to redox cycling unless otherwise indicated. The UV/visible spectra of $DMSOR_{rc}$ samples were highly reproducible, and deconvolution (*15*) confirmed there was negligible contamination with other enzyme forms. Unless otherwise stated, all experiments were performed in 50 mM Tris-Cl^- buffer, containing 1 mM EDTA, pH 8.0. Forward and backward assays were according to the standard procedures of ref (*23*), DMSeO, DMSe, TMAO, or TMA being substituted for DMSO or DMS when appropriate.

Reactions of DMSOR with or in the Presence of DMS. Brief aerobic treatment of DMSOR with DMS, e.g., with 10 mM DMS (Aldrich; added as a solution in ethanol), for up to 10 min at 20 °C was employed to prepare the 'DMS species'. Longer exposure was avoided since this progressively converts this enzyme form to $DMSOR_{mod}D$. The latter was prepared (*15*) by aerobic exposure to DMS at 25 °C for 20 h or more, until the spectral change characteristic of this reaction appeared complete.

For gel-filtration of the DMS species, DMSOR (∼40−60 μM) was treated with DMS (∼100 mM) for a few minutes at about 20 °C in a glovebox (∼5 ppm of O_2), and the sample (∼130 μL) was immediately gel-filtered anaerobically into buffer on a Sephadex G10 column (7 × 45 mm) and the eluate transferred to a spectrophotometer cell. This was sealed and removed from the box, and the spectrum was recorded 10 min after DMS addition. To facilitate anaerobiosis, just prior to use of the column, a portion of $Na_2S_2O_4$ solution was passed through it, and it was then washed with a minimum quantity of anaerobic buffer. The same procedure was used for an analogous experiment in which, in place of treatment with DMS, the enzyme was reduced with $Na_2S_2O_4$ in the presence of MV (final concentrations ∼0.3 and ∼0.6 mM, respectively).

Reactions with DMSe and DMSeO. DMSe (Alpha Aesar) was used as a 1 M stock solution in ethanol or acetone. DMSe was converted to DMSeO by oxidation (cf. *25*, *26*) of a 0.1 M solution in aqueous acetone with a small excess of H_2O_2, removing the excess with catalase. The product was not isolated. In a control experiment, a DMSO solution was

analogously prepared from DMS, and behaved indistinguishably from pure DMSO when substituted for it in forward DMSOR assays.

Spectrophotometric Nernst Titrations of DMSOR with DMS and DMSO. Experiments were performed in a spectrophotometer cell with no gas space, making additions with syringes as for redox cycling (*15*). The spectrum of the enzyme (~30 μM) in the presence of MV (200 μM) was recorded first. $Na_2S_2O_4$ was then added until anaerobiosis was achieved and a small excess of $MV^{\bullet}$ remained, the concentration of which was estimated spectrophotometrically. A known amount of DMSO was added, and the enzyme spectrum was again recorded. Successive further additions of known amounts either of DMSO or of $Na_2S_2O_4$ were then made, the spectrum being recorded again after each addition. The $Na_2S_2O_4$ solution was standardized by titration with $K_3[Fe(CN)_6]$, with MV as indicator. DMS concentrations were calculated on the basis of 1 mol of DMS produced from 2 mol of $MV^{\bullet}$ and 1 mol of DMS from 1 mol of $Na_2S_2O_4$. DMSO concentrations were corrected for its consumption by conversion to DMS. Relative amounts of the oxidized enzyme and of the DMS species were estimated by deconvolution of the spectra as described earlier (*15*), using appropriate reference spectra.

EPR Samples and Measurements. Samples for EPR were prepared by appropriate additions to DMSOR (50−110 μM) in silica tubes, followed by freezing in liquid nitrogen ~2 min after mixing. Anaerobic experiments were performed in a glovebox. Anaerobic oxidation of the DMS species (from 50 μM DMSOR; 2 mM DMS) was with 20 μM DCPIP in the presence of 2 μM PES in 50 mM Tris-Cl^- buffer containing 1 mM EDTA, pH 8.0. For anaerobic reduction of DMSOR with $BV^{\bullet}$, the reductant was prepared by controlled reduction of BV with $Na_2S_2O_4$ and standardized spectrophotometrically. The experiment was performed in 100 mM Na^+-Mes buffer, containing 1 mM EDTA, pH 6.2, using 110 μM DMSOR and 110 μM $BV^{\bullet}$. EPR spectra were recorded on frozen samples, on a Bruker ESP300 spectrometer equipped with a microwave frequency counter and an NMR Gaussmeter. Spectra were manipulated and simulated as described previously (*27*). Cu^{2+}-EDTA was used as the integration standard. Parallel mode EPR measurements were made on a modified Bruker ER 200D-SRC spectrometer equipped with a dual mode cavity and an Oxford Instruments ESR900 liquid helium cooling system. DMSOR was 80 μM, and running conditions were the following: 50 scans of 42 s duration from 10 to 510 mT, modulation amplitude 0.47 mT at 100 kHz, microwave power 2.0 mW, microwave frequency 9.438 GHz, temperature 80 K.

Crystallization and Structure Determination. Crystals for diffraction experiments were obtained at 20−22 °C using $DMSOR_{mod}D$ protein. A solution of the enzyme in 50 mM Tris buffer, pH 8.0, was equilibrated by vapor diffusion against 100 mM Na^+-Hepes, pH 7.5, 2 M $(NH_4)_2SO_4$, and 3−4% PEG400. These crystallization conditions are the same as those reported by Bray et al. (*15*) and yield crystals with the space group $P2_12_12_1$ and unit cell dimensions $a = 67.8$ Å, $b = 116.1$ Å, $c = 230.4$ Å, with two molecules in the asymmetric unit. Crystals grew very quickly, and after 48 h, a single crystal was transferred into mother liquor containing 20% glycerol for 1 min and frozen at 100 K using an Oxford Cryosystems Cryostream.

X-ray diffraction data were collected from the frozen crystal on Station 9.6 of the Synchrotron Radiation Source, CCLRC, Daresbury Laboratory, with X-rays at $\lambda = 0.87$ Å. The detector was an ADSC CCD system. Data were processed using the MOSFLM suite of programs (*28*), and subsequent processing was done using programs from the CCP4 suite (*29*). The program O (*30*) was used for interpretation of electron density maps and model building. The initial model for refinement was a 2.4 Å resolution structure of the native oxidized DMSOR [structure I of ref (*15*)]. Atomic positions and individual atomic temperature factors were refined with the program REFMAC (*31*) using medium noncrystallographic restraints and weak restraints applied to the metal−ligand distances. The same reflections were used for calculation of the free *R*-factor as had been used for the native (oxidized) enzyme structure. σ_A-weighted electron density maps were then calculated using the coefficients $2mF_o-dF_c$, α_{calc} and mF_o-dF_c, α_{calc} (where F_o and F_c represent the observed and calculated structure factors, respectively). After several rounds of refinement and inspection of the model, the refinement was terminated with a crystallographic *R*-factor of 15.8% (see below, Table 2). The current model consists of 2 molecules each comprising residues 3−380 and 394−781, 2 MGD cofactors, and 1 Mo(VI) ion, and solvent molecules comprising 2 sulfate ions and 1200 water molecules (total 6524 atoms). The two molecules in the asymmetric unit were found to be very similar, both in terms of the polypeptide chain (rmsd of 0.20 Å for 741 Cα, excluding 22 Cα atoms affected by intermolecular interactions), and in terms of the molybdenum coordination sphere. Comparisons (see Results) with other forms of the enzyme used only one of the $DMSOR_{mod}D$ molecules, corresponding to chain A in the deposited coordinates.

RESULTS

Effect on the DMS Species of Anaerobic Gel-Filtration. The presumption in earlier work (*11*, *19*−*21*, *23*) is that the DMS species represents a complex of the reduced [Mo(IV)] enzyme with DMSO. If this is the case, then on removal of DMS and DMSO, e.g., by gel-filtration, the enzyme should yield the normal reduced enzyme form. The latter, originally generated by reduction with $Na_2S_2O_4$ and separated by anaerobic gel-filtration, is reported to be autoxidizible (*1*), and its spectrum is quite different from that of the DMS species (see Figure 1). The earlier finding (*23*) that aerobic gel-filtration of the DMS species yielded the spectrum of normal oxidized enzyme could thus be due to air oxidation of a reduced enzyme form. We therefore examined the spectrum of the DMS species following anaerobic gel-filtration to see whether this corresponded to that of the reduced or the oxidized enzyme. Clearly the spectrum (Figure 1) after anaerobic gel-filtration, following treatment with DMS, is essentially that of the resting enzyme [compare curves (a), (b), and (c)]. In contrast, in the parallel experiment in which the enzyme was reduced with $MV^{\bullet}$ and $Na_2S_2O_4$, the reduced spectrum was obtained [curve (d)]. Quantitative analysis (data not shown) of the spectra by deconvolution procedures (*15*) confirmed the above major points. In particular, it provided evidence for no more than a minor contribution of the reduced enzyme spectrum to curve (c).

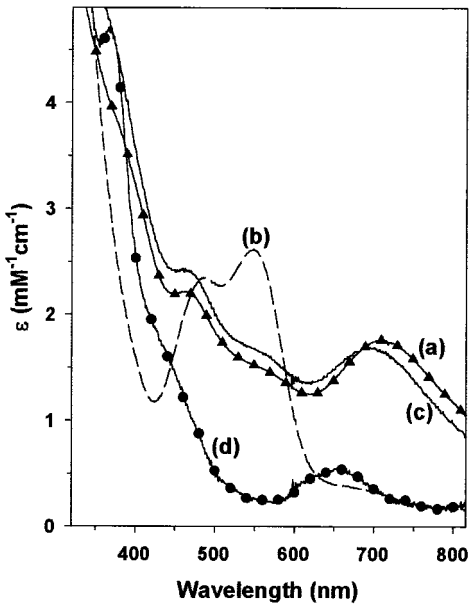

FIGURE 1: Effects of different treatments on the UV/visible spectrum of DMSOR. Curve (a) (with triangle markers), untreated enzyme; curve (b) (dashed line), a sample a few minutes after addition of excess DMS; curve (c) (continuous line), a sample similarly treated anaerobically with DMS and then gel-filtered, also anaerobically; curve (d) (with circle markers), a sample reduced anaerobically with $Na_2S_2O_4$ and MV and then gel-filtered, again anaerobically. Spectra are scaled to correspond approximately to millimolar absorption coefficients; enzyme concentrations ranged from 80 μM [for (a)] to 7 μM [for (d)]. $DMSOR_{ap}$ was used except for curve (b), for which $DMSOR_{rc}$ was used.

There are, however, indications of minor conversion to the $DMSOR_{mod}D$ form [see shift to shorter wavelengths of the long-wavelength peak between curves (a) and (c)].

Equilibria between DMSOR, DMS, and DMSO. During the course of redox cycling DMSOR samples (i.e., reduction by $MV^{\bullet}$ followed by reoxidation by DMSO), we examined the spectrum of the product, without removing the sample from the spectrophotometer cell in which the reactions were carried out. The spectrum was not that of the free oxidized enzyme but of a mixture of this and the DMS species, with the latter often predominating; cf. the dashed red curve of Figure 2(a). After opening the cell and aerobic gel-filtration of the enzyme into buffer, the spectrum changed to that of $DMSOR_{rc}$. Coupled with the established kinetic competence of the DMS species (*23*), this constitutes clear evidence that the latter is the immediate product of the forward turnover reaction.

Adams et al. (*23*) reported that DMSO binds to the oxidized enzyme, causing a small but well-defined change in the UV/visible spectrum. A dissociation constant for this reaction was estimated from equilibrium measurements. Also, using stopped-flow spectrophotometry, an apparent dissociation constant for the reaction of DMS to yield the DMS species was estimated from the forward and reverse rate constants. These workers further reported (*23*) that the DMS species reverts, on a millisecond time scale, to the oxidized enzyme on addition of excess of DMSO. An unexplained finding was that this reaction appeared incomplete under all conditions tested.

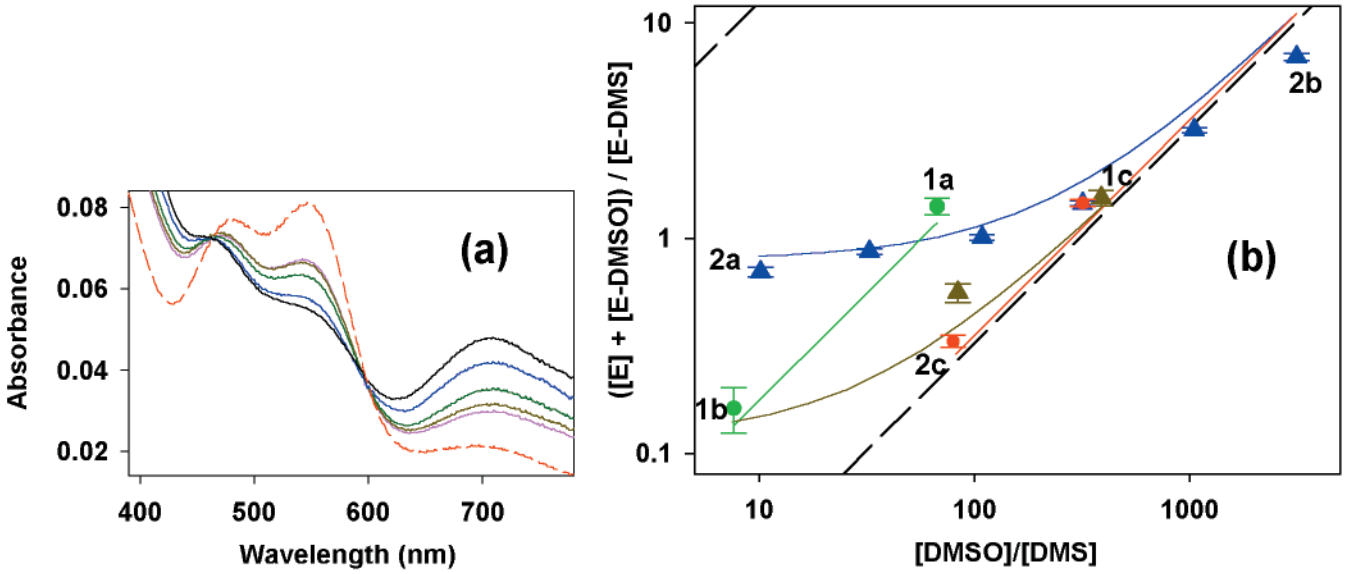

FIGURE 2: Equilibria between DMSOR, DMS, and DMSO. (a) Shows UV/visible spectra at selected points during the titrations, carried out as described under Materials and Methods, DMS being generated in situ by the addition of known amounts of $Na_2S_2O_4$. (b) is the corresponding Nernst plot showing the relative amounts (with errors) of the enzyme species, estimated by deconvolution of the spectra and plotted on a log/log scale as the concentration ratio, [free enzyme + DMSO-complexed]/[DMS species], against [DMSO]/[DMS]. All points correspond to experimental values, and all curves were calculated as described in the text, with $K_o = 21.0$ mM and $K_r = 0.0687$ mM (eq 2). The green points and theoretical curve correspond to titration with DMS of a sample of enzyme in the presence of 4.8 mM DMSO from point 1a to point 1b. The ochre points and curve correspond to further titration of this sample in the presence of 0.6 mM DMS, by two additions of DMSO, from point 1b to point 1c. The blue points and curve show titration of another enzyme sample in the presence of 0.087 mM DMS, by five additions of DMSO, from point 2a to point 2b. The red points and curve correspond to its further titration with DMS (two additions) in the presence of 273 mM DMSO from point 2b to point 2c. The dashed black line toward the right corresponds to the equilibrium limit for saturating concentrations of DMS and DMSO. The dashed black line toward the left shows predicted Mo(VI)/Mo(IV) ratios at the indicated DMSO/DMS ratios, calculated on the basis of EPR data in the literature (see Discussion). In (a), the five continuous curves are spectra from the 2a to 2b series of (b), shown after baseline correction and scaling to correct for dilutions; the dashed red curve shows the spectrum of a separate sample, recorded in a preparative redox-cycling experiment, again after baseline correction and after scaling by a factor of $\times$ 0.35 to correct for the higher concentration.

We investigated the equilibria between the enzyme, DMS, and DMSO. The extreme volatility of DMS (*9*) necessitates the use of a closed system for such work, but even then the quantitation of DMS concentrations is difficult. We therefore generated DMS in situ from DMSO by the addition of known amounts of $Na_2S_2O_4$ (see Materials and Methods). Results from a number of titrations of the enzyme with DMS in the presence of DMSO and vice versa are summarized in Figure 2. After each addition, the relative amounts of the oxidized enzyme and the DMS species were estimated by deconvolution of the UV/visible spectra, without attempting to distinguish between the free oxidized enzyme and its DMSO complex. Isosbestic points [Figure 2(a)] imply the absence in significant amounts of other species. Furthermore, the estimated sum of the concentrations of the two species remained constant within ~5% throughout the titrations. Owing to minor variations in light scattering (allowed for in the fits), good isosbestic points were maintained only over a limited range of conditions [e.g., in Figure 2(a), the dashed red curve shows minor deviations from the other curves]. However, the deconvolutions additionally provided no evidence at any point for the presence of significant amounts of any other enzyme species, in particular for ones having a spectrum analogous to that of the dithionite-reduced enzyme.

For a simple redox equilibrium between the enzyme and the DMSO/DMS couple, of the form

$$E_{ox} + DMS \rightleftarrows E_{red} + DMSO \qquad (1)$$

Nernstian behavior is expected, yielding a straight line on a log−log plot of the concentration ratio for the enzyme couple versus that for the substrate couple, having unit slope and with a position (relative to the origin at $x = 1$, $y = 1$) corresponding to the equilibrium constant of eq 1 and thus to the redox potential difference between the couples. In Figure 2(b), [free enzyme + DMSO-complexed]/[DMS species] is plotted against [DMSO]/[DMS] on a log−log scale. Though some of the data points approximate the dashed line toward the right of the figure, which has unit slope, clearly many points do not do so. Closer examination of the data reveals a dependence of the relative amounts of the enzyme forms on the absolute substrate concentrations as well as on their ratio. This we attribute, for points lying substantially to the left of the dashed line, to the substrate concentrations being too low to achieve saturation of the enzyme. A more complicated relationship is then required:

$$\underset{p}{\text{E-DMSO}} \quad \underset{\text{DMSO}\ o}{\overset{K_o}{\rightleftarrows}} \quad \underset{1\text{-}p\text{-}q}{\text{E}} \quad \underset{DMS\ r}{\overset{K_r}{\rightleftarrows}} \quad \underset{q}{\text{E-DMS}} \qquad (2)$$

For such a system and with saturation with both substrates, Nernstian behavior is again expected with the position of the line on the log−log plot now corresponding to the overall equilibrium constant, K_o/K_r. More generally at equilibrium, with the substrate concentrations and fractional enzyme concentrations as denoted by the letters p, o, etc. below eq 2, and assuming a stoichiometric excess of the substrates over the enzyme, it can be shown that:

$$([E] + [E{-}DMSO])/[E{-}DMS] = (1 - q)/q$$

Table 1: DMSOR Specificity

substrate couple	forward assay ($MV^{\bullet}$)[a]	forward assay ($BV^{\bullet}$)[a]	backward assay[a]	effect of reduced substrate on spectrum
$(CH_3)_2S/(CH_3)_2SO$	28[b]	14	8[b]	'DMS species'
$(CH_3)_2Se/(CH_3)_2SeO$	−	~18[c]	0	similar but 27 nm blue shift[d]
$(CH_3)_3N/(CH_3)_3NO$	52[c]	−	0	no effect

[a] Catalytic center activity ($s^{-1}/2e^{-}$) under the standard conditions of Adams et al. (*23*), except for relevant substitutions of substrates; TMAO was used at 0.5 mM. [b] Data from Bray et al. (*15*). [c] Corrected for nonenzymatic reaction. [d] See Figure 3; only 40% conversion to this species (~100% conversion with DMS).

where $q = (O - 1)/[(O \times R) - 1]$, with $O = 1 + K_o/o$ and $R = 1 + K_r/r$.

If we equate E−DMS with the DMS species, the above ratio corresponds to the one measured experimentally, namely, [free enzyme + DMSO-complexed]/[DMS species]. Clearly in Figure 2(b), the data points, over a wide range of values of the ratio from 0.16 to 7.0, conform rather well to the theoretical curves calculated from the above relationship, strongly supporting the applicability of eq 2.

Substrate Specificity of DMSOR and the Effects of DMS, DMSe, and TMA on the Spectrum of the Enzyme. It has long been known (*18*, *32*) that in the forward assay, trimethylamine *N*-oxide (TMAO) is an even better substrate for DMSOR than is DMSO. Results in Table 1 show that dimethyl selenoxide (DMSeO) is also a good substrate for the enzyme, though because of a rapid nonenzymatic reaction with methyl viologen it was necessary to use benzyl viologen, which has a higher redox potential, to demonstrate this point. For the backward assay, and in contrast to DMS (*23*), no activity was observed with either dimethyl selenide (DMSe) or trimethylamine (TMA).

As already noted, addition of DMS to DMSOR yields (*11*) the DMS species (λ_{max} = ~480 and ~550 nm). Conversion is apparently quantitative,[2] since little absorption at $\lambda > 630$ nm remains and the main spectral features of the oxidized enzyme including the 720 nm peak are no longer seen. Addition of TMA to DMSOR gave no spectral change (data not shown), but DMSe gave effects similar to, but interestingly different from, those with DMS. Figure 3 compares the spectra of $DMSOR_{rc}$ (a), the DMS species (b), and the corresponding DMSe species (d). The latter has been scaled to correspond to 100% enzyme conversion, though actual conversion was only ~40%. (c) shows the experimental spectrum from which (d) was derived by appropriate scaling, after subtraction of the scaled (a) spectrum.[3] Increasing the DMSe concentration from 40 to 80 mM did not increase conversion to the DMSe species significantly (data not shown). The absorption peaks in (b) and (d) are at 548 and 521 nm, respectively. Thus, for the DMSe species in

[2] As in Figure 3 curve (b), the spectrum of the DMS species invariably shows weak residual absorption extending to long wavelengths. We have not determined whether this is a genuine feature of the spectrum of the DMS species, or whether it is due to enzyme conversion to this form being only ~90−95% complete.

[3] Though the main features of the spectrum of the DMSe species are not in doubt, the possibility cannot be excluded that the starting spectrum has been slightly over-subtracted in Figure 3 curve (d), and that in reality some weak long-wavelength absorption features are present.

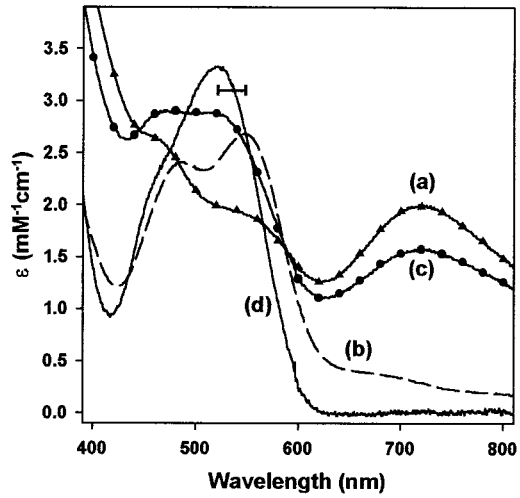

FIGURE 3: Comparison of spectra, plotted as millimolar absorption coefficients, obtained by treating DMSOR with DMS or with DMSe. Spectra are as follows: (a) (with triangle markers), untreated enzyme ($DMSOR_{rc}$); (b) (dashed line), the DMS species (recorded a few minutes after addition of 100 mM DMS to $DMSOR_{rc}$); (c) (with circle markers), the corresponding spectrum obtained under analogous conditions with 40 mM DMS. Since obvious features of the untreated enzyme remain in the latter spectrum, the DMSe spectrum is shown again, (d) (unmarked line), after appropriate subtraction of the scaled (a) untreated enzyme spectrum, followed by rescaling so as to correspond to 100% conversion to the DMSe species, though actual conversion was only about 40%. The horizontal bar indicates the shift in the position of the peak from 548 nm in the DMS species to 521 nm in the DMSe species.

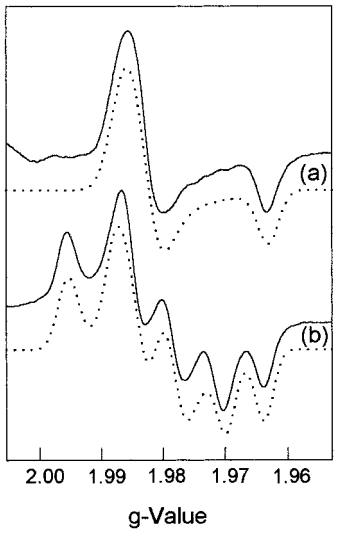

FIGURE 4: Mo(V) EPR spectra from DMSOR samples following different treatments and showing: (a) enzyme after treatment with DMS to give the DMS species, followed by the addition of stoichiometric DCPIP plus PES; and (b) enzyme after reduction with stoichiometric $BV^{\bullet}$. The solid lines show the experimental spectra and the dotted lines simulations, using parameters as follows: for (a), $g_1 = 1.9864$, $g_2 = 1.9823$, $g_3 = 1.9631$; for (b), $g_1 = 1.9915$, $g_2 = 1.9810$, $g_3 = 1.9668$, $A(^1H)_1 = 1.30$, $A(^1H)_2 = 0.99$, $A(^1H)_3 = 1.05$ mT. Samples were prepared as described under Materials and Methods. Recording conditions (giving slight overmodulation) were: temperature, 150 K; microwave power, 5 mW; modulation amplitude, 0.39 mT; microwave frequency, 9.343 GHz.

comparison with the DMS species, the molar absorption coefficient is increased slightly, while conversion to it is decreased from ~100% to ~40%, with the long-wavelength peak shifted 27 nm to shorter wavelengths. The significance of this spectral shift is considered under Discussion.

As for DMS, the spectral change elicited by DMSe was reversed by gel-filtration, the spectrum reverting to that of the normal oxidized enzyme. Also, on standing in air, the spectrum of the enzyme treated with DMSe slowly reverted to that of the normal oxidized enzyme. This behavior contrasts with that of the DMS species, which is slowly converted (*23*) by air to the modified form, $DMSOR_{mod}D$.

EPR Measurements. In early work (*18*), a considerable number of well-defined Mo(V) EPR signals from the enzyme were described in detail. However, precise conditions for obtaining the signals were not specified. In the present work, to relate EPR parameters to available structural information, we examined enzyme samples prepared under well-defined conditions. Untreated $DMSOR_{rc}$ gave only very weak signals, as did samples to which DMS had been added to convert the enzyme to the DMS species. Also, in parallel mode EPR, only weak signals were detected, with no significant differences between samples of the DMS species and those of the enzyme alone, both under the recording conditions given under Materials and Methods and also (though with smaller numbers of scans) at temperatures down to 4 K and at fields up to 1.1 T.

Anaerobic treatment of the DMS species with a stoichiometric $1e^-$ equiv of the redox dyes used in the backward assay (DCPIP plus a smaller amount of PES) yielded a well-defined EPR signal, with no indications of coupling to protons [Figure 4(a)]. Conversion to the Mo(V) state was 3%, and the parameters of the signal obtained by simulation were indistinguishable from those reported (*18*) for the High-g Unsplit type 2 signal. Conversely, reduction of $DMSOR_{rc}$ samples by using a stoichiometric $1e^-$ equiv of viologen radical yielded a signal again corresponding to 3% conversion to the Mo(V) state, but with obvious hyperfine splittings, no doubt from coupling to ^1H nuclei [Figure 4(b)]. The medium used (MES buffer, pH 6.2) was analogous to that in an earlier nonstoichiometric experiment (*18*), and a well-defined signal, the High-g Split (Mes) signal, was obtained. Parameters from the simulation [caption to Figure 4(b)] are scarcely distinguishable from the earlier values for the signal in this medium.

Steady-State Kinetics: Forward Assay. Adams et al. (*23*) reported a number of parameters relating to the forward assay of DMSOR with DMSO and $MV^{\bullet}$. Under the conditions of these workers, additional data were obtained on the effect of variations in the concentration of DMSO. Relative to the standard assay with 5 mM DMSO, no inhibition was observed with DMSO up to 200 mM. Though precise estimation of the apparent K_m for DMSO was difficult, assays with decreased DMSO concentrations indicated a value for this parameter <50 μM and probably ~10 μM.

Preparation of $DMSOR_{mod}D$. The reaction of DMSOR with DMS to form the DMS species is very fast with an apparent first-order rate constant >500 s^{-1} at pH 8.0 and 10 °C (*23*). On longer aerobic, but not anaerobic, exposure to DMS, this species progressively becomes converted to $DMSOR_{mod}D$ (*15*, *23*). The data in Figure 5(a) show clear isosbestic points, implying no detectable intermediates in this reaction. Further data (not shown) indicate a complex dependence on the oxygen concentration, with estimates of the apparent first-order rate constant at different stages of the reaction ranging from 0.17 to 0.40 h^{-1}.

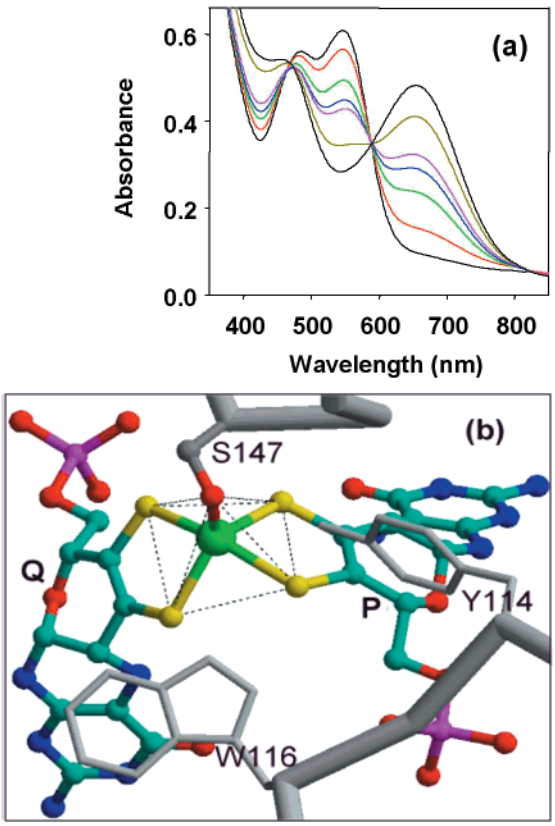

FIGURE 5: (a) Spectra recorded at intervals during the aerobic conversion of DMS-treated enzyme into $DMSOR_{mod}D$ and showing isosbestic points. (b) Structure of the molybdenum site of $DMSOR_{mod}D$ determined by X-ray crystallography. In (a), the curves (black, red, green, blue, pink, ochre, and black) correspond to the following reaction times: 0.01, 0.76, 2.9, 5.4, 7.8, 28, and 46 h. The experiment was carried out aerobically in 100 mM $Tris\text{-}Cl^-$, 1 mM EDTA, pH 8.0 at 25 °C, with 200 μM enzyme and 100 mM DMS. After 24 h, though the spectral change appeared incomplete, the reaction had become slow probably because of O_2 depletion, and the experiment was therefore interrupted, the sample was gel-filtered and reconcentrated, and a further portion of DMS was added. Spectra in the second part of the experiment have been scaled by a factor of × 0.945 to compensate for the different enzyme concentrations. No baseline corrections were applied. In (b), the dashed black line indicates the approximately tetrahedral coordination to molybdenum of the four thiolate ligands from the P and Q MGD molecules and the oxygen from Ser-147. The thick gray line indicates sections of the peptide backbone. Thin gray lines indicate residues Tyr-114 and Trp-116.

Structure of the $DMSOR_{mod}D$ Form of the Enzyme. Crystals of $DMSOR_{mod}D$ were obtained, and the structure was determined as described under Materials and Methods and in Table 2. The refined model of $DMSOR_{mod}D$ was compared with previously determined structures of the oxidized enzyme: $DMSOR_{ap}$ crystallized under different conditions [ref (*12*), in the presence of sodium citrate buffer], and $DMSOR_{ap}$ crystallized from the same conditions as $DMSOR_{mod}D$ [structure II of ref (*15*), in the presence of Na^+-Hepes buffer] and converted to the $DMSOR_{mod}H$ form during the process. Superposition of the polypeptide chain of $DMSOR_{mod}D$ on that of $DMSOR_{ap}$ demonstrates the structures are similar with an rmsd of 0.29 Å for 763 Cα. Similarly, $DMSOR_{mod}D$ could be superimposed on $DMSOR_{mod}H$ with an rmsd of 0.17 Å for 763 Cα. That the latter value is slightly lower than the former suggests that the crystallization conditions do have a small effect on the polypeptide chain. Although the polypeptide chain of $DMSOR_{mod}D$ is more similar to that of $DMSOR_{mod}H$, examination of the molybdenum binding site demonstrates that the position of the metal in $DMSOR_{mod}D$ is closer to that observed for $DMSOR_{ap}$ (*12*) with respect to the thiolate ligands donated by the molybdopterin cofactors. Superposition of the MGD and the molybdenum of $DMSO_{mod}D$ and $DMSOR_{ap}$ indicates only a small movement of the Mo atom of 0.2 Å relative to the pyranopterin moieties. Previously we have shown that aerobic exposure to Hepes buffer can cause a large (1.4 Å), time-dependent movement in the position of the molybdenum relative to the thiolate ligands. Thus, Hepes buffer, in agreement with our earlier conclusions from spectrophotometry (*15*) and in contrast to its effects on $DMSOR_{ap}$, has no specific destabilizing effect on $DMSOR_{mod}D$.

Table 2: $DMSOR_{mod}D$: Data Collection and Refinement[a]

Data Collection and Processing Statistics	
resolution (Å)	2.0
R_{sym}[b] (2.10−1.99 Å)	0.042 (0.071)
no. of observations	277682
no. of unique reflections	105657
% complete (2.10−1.99 Å)	83.7 (49.2)
$\langle I\rangle/\langle\sigma I\rangle$ (2.10−1.99 Å)	11.3 (9.0)
Refinement Statistics	
resolution (Å)	20−2.0
no. of atoms	13171
R-factor (%)[c]	15.8
R-free (%)[d]	20.9
rmsd[e] bond lengths	0.013
rmsd[e] bond angles	1.7

[a] Approximate age of crystals, 48 h; cryoprotectant, 20% glycerol. [b] $R_{sym} = \Sigma|I(k) - \langle I\rangle|/\Sigma I(k)$ where $I(k)$ and $\langle I\rangle$ represent the diffraction intensity values of individual measurements and the corresponding mean values. σ represents the standard deviation. [c] *R*-factor $= \Sigma|F_o - F_c|/\Sigma F_o$ where F_o and F_c are the observed and calculated structure factor amplitudes. 95% of the data were used for refinement and included in the calculation of *R*-factor. [d] *R*-free = *R*-factor calculated for 5% of reflections not included in refinement. [e] rmsd = root-mean-square deviation from ideality.

The electron density at the metal center of $DMSOR_{mod}D$ is consistent with only five ligands to the Mo, as illustrated in Figure 5(b). The four sulfurs donated by the two molybdopterin cofactors are at a distance of 2.4−2.5 Å from the metal, and Oγ of Ser147 is at 1.9 Å. The geometry of the metal site is slightly distorted square pyramidal, with four sulfurs at the base and Oγ of Ser147 at the apex [Figure 5(b)]. Changes in the oxygen ligation of the metal observed in the $DMSOR_{mod}D$ structure, compared with $DMSOR_{ap}$ (*12*) and $DMSOR_{mod}H$, appear to have an effect on regions of the polypeptide chain centered on Ser147, the molybdenum ligand. The density of residues 140−150, 111−114, and 394−399 is very poor, and this is reflected by raised temperature factors for atoms in these residues. The *B*-factors of residues 140−150 are 3−4-fold higher than the *B*-factors of the same residues in structures of the oxidized enzyme (*12*, *15*). The effect is also observed in residues 111−114 and 394−399, which have an approximate 2-fold increase in *B*-factors and which are involved in main chain hydrogen bonds to residues 140−150. We interpret this to mean that the absence of an oxo ligand to the molybdenum in its oxidized state enhances local mobility of the Ser147 ligand, which is transmitted to surrounding residues.

Table 3: Wavelength Shifts on Replacing S by Se, Redox Potentials, and the Structure of the DMS Species

no.	redox couple, or complex/ *structure after hypothetical transfer of charge*[a]	ref	effect of replacing S by Se: redox potential (source)	effect of replacing S by Se: λ_{max} shift, predicted[b]	effect of replacing S by Se: λ_{max} shift, observed
I	$(Me)_2S/(Me)_2S^{\bullet+}$ [redox couple]	(*35*)[2]	↓		
II	$(Me)_2SO^{\bullet-}/(Me)_2SO$ [redox couple]	(*35*)[2]	↑		
III	$[(NH_3)_5Ru^{III}S(CH_3)_2]^{3+}/[(NH_3)_5Ru^{II}S^{\bullet+}(CH_3)_2]^{3+}$ [LMCT]	(*37*)	↓ (assumed[c])	↑	↑
A	$Mo^{VI}{=}O\cdots S(Me)_2/Mo^{V}-O-S^{\bullet}(Me)_2$ [LMCT]	present work	↓ (from I)	↑	↓
B1	$Mo^{V}-O-S^{\bullet}(Me)_2/\ Mo^{VI}{=}O\cdots S(Me)_2$ [MLCT]	present work	↓ (from I)	↓	↓
B2	$Mo^{V}-O-S^{\bullet}(Me)_2/Mo^{IV}\cdots O{=}S(Me)_2$ [LMCT]	present work	↑ (from II)	↓	↓
C	$Mo^{IV}\cdots O{=}S(Me)_2/Mo^{V}-O-S^{\bullet}(Me)_2$ [MLCT]	present work	↑ (from II)	↑	↓

[a] I and II are known redox couples, and III is a known complex with, in italics, the corresponding structure after hypothetical transfer of negative charge. A, B1, B2, and C are suggested structures for the DMS species, also with, in italics, the corresponding structures after those hypothetical charge transfers that are possible. [b] Predicted from nature of the charge transfer and the redox potential information. [c] Data from I were not available at the time of (*37*).

DISCUSSION

The Nature of the DMS Species: Earlier Structural and Spectroscopic Data. The earlier presumption, based on a number of sources (*20*, *21*), was that the DMS species represents a complex of the reduced [Mo(IV)] enzyme with DMSO. In the crystal structure of DMS-treated enzyme, the DMS residue is clearly seen (*11*) with its sulfur atom bonded, at a distance of 1.7 Å, to an oxygen atom, 'O2' of the oxidized structure, which in turn is 2.0 Å from molybdenum. This oxygen is 0.2 Å further from the metal in this complex, than is the corresponding oxygen of the free enzyme (*12*). Raman data (*21*) on the DMS species, recently confirmed independently (*22*), are consistent, indicating a bond order of approximately 1.5 for the oxygen−sulfur linkage and a single bond for molybdenum−oxygen. EXAFS work by George and co-workers (*19*) also appeared consistent. Though the X-ray absorption edge position (*20*) was claimed to indicate Mo(IV), the data are scarcely definitive (*19*, *33*). Furthermore, remeasurement of the Mo X-ray edge position of the DMS species by B. Bennett and C. D. Garner, indicating (personal communication) that Mo(IV) is unlikely, suggested to us that re-assessment of the DMS species might be needed. The UV/visible spectrum of the DMS species can in principle also provide information on the oxidation state of the metal, and it has been claimed (*21*) that the 550 nm band is due to metal-to-ligand charge transfer in a Mo(IV) species. Though progress has been made through model compound work (e.g., *34*) in understanding the spectrum of the oxidized enzyme, this does not extend to the DMS species. The marked difference between the spectrum of the latter and that of the dithionite-reduced Mo(IV) enzyme form thus remains to be fully explained.

The Nature of the DMS Species: Equilibrium Data. The present work has confirmed the conclusion (*23*) that reaction of DMSOR with DMS to yield the DMS species is readily reversible, extending it to reversal by gel-filtration performed anaerobically. Furthermore, that the equilibria between the enzyme, DMS, and DMSO, investigated in Figure 2, conform to eq 2 rather than to eq 1 emphasizes the necessity for binding of the substrates to the enzyme before any reaction can occur. These data provide no information on the redox state of the enzyme or the bound substrate molecule in the complex written as E−DMS in eq 2 that we equate with the DMS species. In E and E−DMSO, however, there can be little doubt that the metal is Mo(VI). The value, $K_o/K_r = 306$ [Figure 2(b)], corresponds to a difference between the substrate and enzyme redox potential couples of 74 mV (for a $2e^-$ reaction at 25 °C and pH 8.0). According to Wood (*9*), the DMSO/DMS potential at this pH value is 101 mV. Thus, the redox potential for conversion of the DMSO complex of the enzyme to the DMS complex is 175 mV at pH 8.0. For comparison, the Mo(VI)/Mo(IV) redox potential for the free enzyme has been estimated by EPR titrations at pH 7.0 (*1*) and at pH 8.5 (*19*). Combining these two sources which agree closely with one another, averaging the two $1e^-$ potentials to yield the $2e^-$ potential, and correcting to pH 8.0 (on the basis of 59 mV/pH unit) give a value for the $2e^-$ reduction of molybdenum of the enzyme of 98 ± 12 mV. Thus, the overall substrate displacement reaction of eq 2 takes place at a potential some 80 mV higher than that reported for molybdenum reduction (see the dashed lines in Figure 2).[4] The data therefore make questionable the widely accepted assumption that reaction of the enzyme with DMS to give the DMS species is a reaction closely analogous to the $2e^-$ reduction of molybdenum in the free enzyme.

The Nature of the DMS Species: The Significance of the 27 nm Shift to Shorter Wavelengths in the DMSe Species. From its intensity ($\epsilon = 2.5\ mM^{-1}\ cm^{-1}$), the absorption band at ~550 nm of the DMS species is presumably of charge transfer origin. Changing a ligand atom to one having a higher or a lower redox potential, while noting the direction in which the relevant absorption band shifts, is a tool routinely used for distinguishing between LMCT (ligand-to-metal charge transfer) and MLCT (metal-to-ligand charge transfer) bands. A shift to shorter wavelengths identifies a band as due to MLCT if replacing S by Se lowers the redox potential of the coordinated ligand, but to LMCT, if such a change raises it.

In Table 3, data on the effects of replacing S by Se in some relevant models (*35*, *37*, *38*) are compared with the

[4] A referee has raised the question of whether the discrepancy between the literature Mo redox potential from EPR and the present value from spectrophotometry relative to the DMS/DMSO potential (*9*) might be due to experimental differences. While we cannot exclude this rigorously, we think it unlikely for the following reasons. The theoretically determined DMS/DMSO potential was originally quoted as being accurate to within 5 mV (*9*) and has been widely accepted [e.g., (*35*, *36*)]. Three determinations of the Mo potential, including measurements on both liquid and frozen samples, have all given quite similar values (*1*, *17*, *19*). Furthermore, for the homologous DMSOR from *E. coli*, which retains the serine ligand of Mo, redox potentials (*36*) are some 200 mV lower than these values for the *R. capsulatus* enzyme, a finding tending to point toward a lower rather than a higher Mo potential in the latter.

predicted effects of such replacement, for three different structures that might be envisaged for the DMS species. From pulse radiolysis (*35*), for the 1e$^-$ oxidation of DMS, replacing S by Se results in a decrease in redox potential, but for the 1e$^-$ reduction of DMSO there is an increase[5] (Table 3). It is reasonable to assume that such redox potential changes hold also for DMS and DMSe when bound in metal ion complexes, and, indeed, data in support of this are available. Thus, for ammine Ru(III) complexes of DMS and DMSe (*37*), consistent with a decrease in the ligand redox potential on changing from S to Se and as expected for LMCT, there is a wavelength shift of the band at 453 nm to 487 nm (Table 3). For the DMS species, on the other hand, the observed shift is to shorter wavelengths. In the three possible structures, A, B, and C, suggested for this species (Table 3), zero, one, or two electrons, respectively, have been transferred from the bound substrate to the metal ion. As shown in Table 3, again accepting that the redox potentials cited remain applicable to the coordinated species that we are observing, neither the Mo(VI)−DMS complex A nor the Mo(IV)−DMSO complex C, advocated by Garton et al. (*21*), is consistent with the observed shift to shorter wavelengths. Thus, by default, we are left with the Mo(V)/S radical formulation B, for which not only MLCT (B1) but also LMCT (B2) would result in the observed spectral shift. In view of the high redox potential at which formation of the DMS species occurs, the former appears more probable.

Thus, the wavelength shift appears positively to identify the band as arising from charge transfer in a Mo(V)/S radical species. The DMS species gives no EPR signal either in normal mode [(*20*); confirmed in the present work] or in parallel mode. This implies that if molybdenum is indeed Mo(V), there must be a free radical in close proximity to the metal and interacting strongly with it, as for a Mo^V−O−S$^\bullet$Me$_2$ structure. Available crystallographic (*11*), Raman (*21*, *22*), and EXAFS (*19*) data appear compatible with such a structure. In further support, in recent model compound work, Holm and co-workers (*39*) encountered both Mo(V) species and radicals. Specifically, in apparent analogy with the tungsten DMSOR (*17*, *40*), a des-oxo W(IV) complex, [W^{IV}(OPh)(S$_2$C$_2$Me$_2$)$_2$]$^{1-}$, accepted the oxo group from DMSO to give the corresponding W(VI) oxo complex. However, for the analogous Mo complex, while the corresponding reaction apparently occurred, the final product was nevertheless a Mo(V) species, believed to arise via an internal redox reaction and decay of a radical intermediate.

The Structure and Nature of DMSOR$_{mod}$D. In the structure of DMSOR$_{mod}$D [Figure 5(b)], the molybdenum lacks any oxygen ligands[6] other than that from serine-147. All four dithiolene sulfur ligands are coordinated. This structure contrasts with that of the other oxygen-damaged form, DMSOR$_{mod}$H, in which a pair of thiolates have dissociated (*15*). From the requirement for oxygen for formation of DMSOR$_{mod}$D, it is likely that the metal is in the Mo(VI) oxidation state, in line with earlier predictions (*23*). Thus, DMSOR$_{mod}$D is a dead-end species in relation to the normal catalytic cycles, since the metal is in the wrong oxidation state to donate electrons to the acceptor, while lacking the oxo ligand needed for oxygen transfer to DMS. This is fully consistent with DMSOR$_{mod}$D being inactive in the backward assay with DMS as reducing substrate. It is equally consistent with its being re-converted (*23*) to the normal enzyme form, with full restoration of this activity, after reduction of the molybdenum during redox cycling.

Scheme 1: Proposed Scheme for DMSOR Action in the Forward (Blue Arrows) and Backward (Magenta and Ochre Arrows) Assays and for Its O_2-Dependent Inactivation (Green Arrows) to DMSOR$_{mod}$H (mh) or DMSOR$_{mod}$D (md)[a]

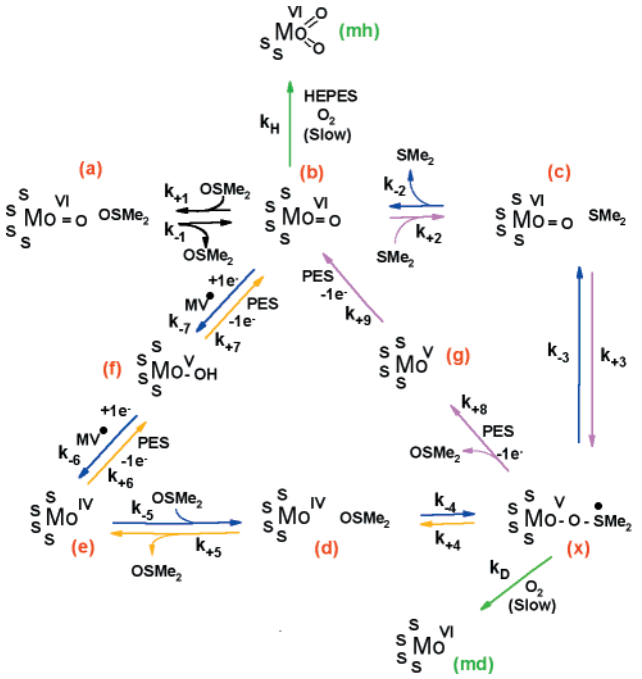

[a] (b) is the resting untreated oxidized enzyme (DMSOR$_{rc}$), (x) is the DMS species, (a), (c), and (d) are noncovalent complexes, (c) and (d) being Michaelis complexes, and (f) and (g), respectively, are the Mo(V) species giving the High-g Split and High-g Unsplit EPR signals. The UV/visible spectrum of (a) is marginally different (*23*) from that of (b). Those of (c) and (d) are assumed to be similar to those of (b) and (e), respectively. As discussed in the text, the PES-mediated steps of the backward assay may involve the pathway denoted by either the magenta or the ochre arrows. For simplicity, the serine ligand of molybdenum is omitted throughout, as are the bonds linking Mo to the thiolate S atoms.

Catalytic Pathways of DMSOR and the Relationships of the Oxygen-Damaged Species to the Species on These Pathways. Scheme 1 summarizes the proposed scheme for DMSOR action in the forward and the backward catalytic reactions, as well as showing the O_2-dependent inactivation reactions that lead to formation of DMSOR$_{mod}$H and DMSOR$_{mod}$D. The catalytic reactions in Scheme 1 are kinetically as proposed by Adams et al. (*23*), and species

[5] From pulse radiolysis work (*35*), chalcogen−oxygen single bond strengths in OH adducts of the R$_2$X chalcogenides increase as one traverses the chalcogens from S to Te, whereas the trend is in the opposite direction for the corresponding chalcogen−oxygen double bonds. Though this work relates mainly to aryl compounds, it is clear that similar considerations apply to the alkyl analogues.

[6] Recent Raman work (*22*) contains the suggestion that DMSOR$_{mod}$D may be a di-oxo form of the enzyme, based on the observation of two Mo═O stretching bands from samples of this enzyme form. The intensity of the bands is not discussed. Furthermore, questions of sample homogeneity clearly arise. Conversion of DMSOR$_{rc}$ to DMSOR$_{mod}$D is accompanied (*23*) by a decrease in the ratio of activity in the backward assay to that in the forward assay. In the original work (*23*), the decrease in this ratio was 98%, whereas in (*22*), it was only 57%, implying that conversion was far from quantitative. [Note that the absolute value of this activity ratio for DMSOR$_{rc}$ in (*22*) is × 3.5 lower than that in (*23*), presumably because of differences in assay conditions.]

(a)−(e) are formulated identically to the corresponding species of these workers. The resting oxidized enzyme [species (b)] is susceptible, at least in the presence of Hepes buffer, to slow oxygen-dependent degradation (reaction k_H) to species (mh). The latter is $DMSOR_{mod}H$, a di-oxo form retaining only two thiolate ligands to the molybdenum (*15*). Adams et al. (*23*) equated the DMS species with species (d). Clearly, however, their formulation of this species as an Mo(IV) form is inconsistent with the new data. Since Mo(IV) DMSOR species certainly do exist, including presumably the Michaelis complex species (d), it therefore becomes necessary to introduce the DMS species into Scheme 1 as an additional form, species (x).

It has previously been assumed (*23*) that the back-assay involves reduction of the enzyme by DMS to the Mo(IV) level, followed by product dissociation and reoxidation of the metal by the dyes PES and DCPIP (as in steps k_{+5}, k_{+6}, and k_{+7}). However, the present data make it questionable whether the Mo(IV) state is involved. EPR and the structure of $DMSOR_{mod}D$ provide additional information on the nature of these reactions. $1e^-$ oxidation of the DMS species [(x) in Scheme 1], formulated as $Mo^V-O-S^{\bullet}(Me)_2$, with reaction occurring preferentially at the sulfur radical, would permit dissociation of the DMSO product (step k_{+8}), leaving a des-oxo Mo(V) enzyme species (g), that should be identifiable by EPR. It is important, therefore, that a well-defined High-g Unsplit type 2 signal was obtained in an experiment designed to examine the product of $1e^-$ oxidation of the DMS species. Consistent with the prediction of a des-oxo Mo(V) enzyme form, this signal, in contrast to the High-g Split EPR signal, lacks splitting from exchangeable protons derived from hydroxyl or water ligands of the metal. On the other hand, we obtained the High-g Split signal on reduction of the enzyme with a stoichiometric quantity of viologen radical (step k_{-7}). The EPR data thus provide clear evidence for the nature of both species (f) and species (g). The relative weakness of both the EPR signals under the experimental conditions does not detract from these conclusions, on the reasonable assumption that steps k_{+9} and step k_{-6} are faster, respectively, than are steps k_{+8} and step k_{-7}.

As an alternative to participating in the catalytic cycle, the DMS species can, in the presence of air and excess DMS, undergo the slow degradative reaction (step k_D) that leads to conversion of DMSOR into $DMSOR_{mod}D$ [species (md)]. Molecular oxygen is known (*23*) not to function significantly as the oxidizing substrate in the backward assay, pointing to a substantial difference between this reaction and the PES-dependent one, step k_{+8}. Formation of $DMSOR_{mod}D$ from the DMS species by reaction k_D is likely to involve two successive $1e^-$ reactions with molecular oxygen. In contrast to the catalytically significant reaction with PES discussed above, oxidation of the metal from the Mo(V) state to Mo(VI) presumably precedes reaction of the sulfur radical and product dissociation.

Specificity and Kinetics of DMSOR Action. DMSOR is active in the forward assay with DMSO, DMSeO, and TMAO. However, under standard conditions in the corresponding backward assays, it is only active with DMS. In the presence of DMSe, DMSOR forms a species spectroscopically analogous to the DMS species, though enzyme conversion is incomplete. No analogous TMA species is detectable. Finally, in contrast to the situation with the DMS species, exposure of the DMSe species to air yields neither $DMSOR_{mod}D$ nor some analogous species, but instead reverts to the normal oxidized enzyme. Redox potential differences among the three substrate couples must be important in relation to these differences. Though fully definitive data are not available, it seems (*9*, *35*, *40*, *41*) that these $2e^-$ potentials decrease in the order DMSeO/DMSe > DMSO/DMS > TMAO/TMA. Thus, though the failure of the enzyme to oxidize DMSe is explicable simply on this basis, other factors must be invoked in the case of TMA. Failure to form a TMA species could arise from instability of the relevant radical compared to those derived from DMS and DMSe, since only the latter have relatively low-lying π-type orbitals available to aid in stability. Incomplete formation of the DMSe species might imply $k_{+3} \sim k_{-3}$ rather than $k_{+3} > k_{-3}$, as is the case for DMS (see below), with this in turn favoring regeneration to the resting enzyme over $DMSOR_{mod}D$ formation.

In relation to the catalytically significant reactions of DMSO and DMS with the enzyme in the absence of PES or of $MV^{\bullet}$, the Nernst data throw new light on the results of Adams et al. (*23*). The equilibrium nature over a wide range of concentrations of the reactions of DMSO and DMS with the enzyme (Figure 2) renders unnecessary the earlier conclusion (*23*) that a DMSOR form exists that is not reoxidizable (or reconvertible to the free enzyme) by DMSO. Importantly, the agreement between the dissociation constants for the binding both of DMSO and of DMS to the oxidized enzyme, with the values determined earlier (*23*) by quite different methods, is striking. Thus, for DMSO binding, the dissociation constant (K_o, eq 2), estimated from the data in Figure 2, was 21 ± 5 mM, indistinguishable from the earlier value (*23*) of 17 ± 4 mM. Similarly, the constant for DMS binding to yield the DMS species (K_r) from Figure 2 is 0.07 ± 0.01 mM, whereas an apparent dissociation constant of 0.13−0.16 mM was calculated from stopped-flow data (*23*). Though caution is necessary in relation to the exact value of K_r, since the latter measurements were at pH 5.5 rather than pH 8.0 and since DMS volatility could have led to its overestimation, such overall agreement gives confidence that the nature of the reactions is as shown in Scheme 1. The scheme is reconciled with eq 2 by taking $K_o = k_{-1}/k_{+1}$; $K_r = (k_{-2}/k_{+2}) \times (k_{-3}/k_{+3})$; $k_{+3} \gg k_{-3}$ (see below); and $k_{-4} \gg k_{+4}$. Reaction of DMS with the enzyme to yield the DMS species is depicted as a two-step reaction, in keeping with earlier stopped-flow data (*23*, *42*). Thus, though at pH 8.0 formation of the DMS species was too fast to measure on the stopped-flow time scale, with a rate constant $>500\ s^{-1}$, reversal by DMSO was slower, with a concentration-independent rate constant of $61\ s^{-1}$. With $k_{+3} > k_{-3}$, the latter value is presumably limited primarily by step k_{-3}. It is tempting to speculate that reactions k_{+3} and k_{-3} are related to the closing and reopening, respectively, of the 'lid' (*13*) containing residue Trp388, that is known (*11*) to enclose the active site in the DMS species.

The DMSO complex [Scheme 1, species (a)] is a dead-end species in relation to enzyme turnover. As such, its formation might result in inhibition of the forward assay at high DMSO concentrations. That no such inhibition was observed implies that $MV^{\bullet}$ can react not only with species (b) but also with species (a), though this is not shown in Scheme 1. Finally, the significance of the two alternative pathways of the back-reaction, via steps k_{+8} and k_{+9}, or steps

k_{+4}, k_{+5}, k_{+6}, and k_{+7}, must be considered. It is highly likely that the former pathway, in which the Mo(IV) state of the enzyme is by-passed, operates at least to some extent. The EPR data clearly demonstrate the existence of step k_{+8}. Furthermore, the Nernst titrations indicate the equilibria, k_{+4}/k_{-4} and k_{+5}/k_{-5}, greatly favor the DMS species (x) over the Mo(IV) species (d) and (e). Nevertheless, it seems that steps k_{+4}, k_{+5}, k_{+6}, and k_{+7} play some part in backward enzyme turnover. DMSO is an effective inhibitor (*23*) of the standard backward assay (50% inhibition for 60 μM DMSO, with 20 mM DMS), a finding perhaps most readily understood in terms of DMSO binding to a Mo(IV) enzyme form, via reaction k_{-5}. Our finding of a low ($\sim$10 μM) apparent K_m for DMSO in the forward assay is in keeping with this.

The k_{+8}, k_{+9} pathway, by-passing the Mo(IV) state, appears not to have been considered by previous workers on the DMSOR from photosynthetic organisms. However, recent electrochemical work (*36*) on the related *E. coli* enzyme drew attention to the importance of considering all the possible alternative redox pathways for enzymes of this type. Existence of the k_{+8}, k_{+9} pathway would imply that the backward and forward assays proceed by different mechanisms. This might in turn have implications in relation to the evolution (*43*) of separate molybdopterin enzymes that catalyze, respectively, DMSO reduction and DMS oxidation.

ACKNOWLEDGMENT

We thank Prof. C. D. Garner and Dr. B. Bennett for giving us information on their unpublished work, Dr. A. G. McEwan for providing the *R. capsulatus* strain used for this work, and Dr. M. Cheesman and Dr. G. Merényi for helpful discussions.

REFERENCES

1. Bastian, N. R., Kay, C. J., Barber, M. J., and Rajagopalan, K. V. (1991) *J. Biol. Chem. 266*, 45−51.
2. McEwan, A. G., Ferguson, S. J., and Jackson, J. B. (1991) *Biochem. J. 274*, 305−307.
3. Czjzek, M., DosSantos, J. P., Pommier, J., Giordano, G., Mejean, V., and Haser, R. (1998) *J. Mol. Biol. 284*, 435−447.
4. Garton, S. D., Temple, C. A., Dhawan, I. K., Barber, M. J., Rajagopalan, K. V., and Johnson, M. K. (2000) *J. Biol. Chem. 275*, 6798−6805.
5. Hille, R. (1996) *Chem. Rev. 96*, 2757−2816.
6. Wootton, J. C., Nicolson, R. E., Cock, J. M., Walters, D. E., Burke, J. F., Doyle, W. A., and Bray, R. C. (1991) *Biochim. Biophys. Acta 1057*, 157−185.
7. Stiefel, E. I. (1996) *Science 272*, 1599−1600.
8. Ayers, G. P., and Gillett, R. W. (2000) *J. Sea Res. 43*, 275−286.
9. Wood, P. M. (1981) *FEBS Lett. 124*, 11−14.
10. Ginzburg, B., Chalifa, I., Zohray, T., Hadas, O., Dor, I., and Lev, O. (1998) *Water Res. 32*, 1789−1800.
11. McAlpine, A. S., McEwan, A. G., and Bailey, S. (1998) *J. Mol. Biol. 275*, 613−623.
12. McAlpine, A. S., McEwan, A. G., Shaw, A. L., and Bailey, S. (1997) *J. Biol. Inorg. Chem. 2*, 690−701.
13. Schindelin, H., Kisker, C., Hilton, J., Rajagopalan, K. V., and Rees, D. C. (1996) *Science 272*, 1615−1621.
14. Schneider, F., Lowe, J., Huber, R., Schindelin, H., Kisker, C., and Knablein, J. (1996) *J. Mol. Biol. 263*, 53−69.
15. Bray, R. C., Adams, B., Smith, A. T., Bennett, B., and Bailey, S. (2000) *Biochemistry 39*, 11258−11269.
16. Li, H.-K., Temple, C., Rajagopalan, K. V., and Schindelin, H. (2000) *J. Am. Chem. Soc. 32*, 7673−7680.
17. Stewart, L. J., Bailey, S., Bennett, B., Charnock, J. M., Garner, C. D., and McAlpine, A. S. (2000) *J. Mol. Biol. 299*, 593−600.
18. Bennett, B., Benson, N., McEwan, A. G., and Bray, R. C. (1994*) Eur. J. Biochem. 225*, 321−331.
19. George, G. N., Hilton, J., Temple, C., Prince, R. C., and Rajagopalan, K. V. (1999) *J. Am. Chem. Soc. 121*, 1256−1266.
20. Baugh, P. E., Garner, C. D., Charnock, J. M., Collison, D., Davies, E. S., McAlpine, A. S., Bailey, S., Lane, I., Hanson, G. R., and McEwan, A. G. (1997) *J. Biol. Inorg. Chem. 2*, 634−643.
21. Garton, S. D., Hilton, J., Oku, H., Crouse, B. R., Rajagopalan, K. V., and Johnson, M. K. (1997) *J. Am. Chem. Soc. 119*, 12906−12916.
22. Bell, A. F., He, X., Ridge, J. P., Hanson, G. R., McEwan, A. G., and Tonge, P. J. (2001) *Biochemistry 40*, 440−448.
23. Adams, B., Smith, A. T., Bailey, S., McEwan, A. G., and Bray, R. C. (1999) *Biochemistry 38*, 8501−8511.
24. Hilton, J. C., Temple, C. A., and Rajagopalan, K. V. (1999) *J. Biol. Chem. 274*, 8428−8436.
25. Peak, D. A., and Watkins, T. I. (1950) *J. Chem. Soc*., 445−452.
26. Cinquini, M., Colonna, S., and Giovini, R. (1969) *Chem. Ind. (London) 27*, 1737.
27. Turner, N. A., Doyle, W. A., Ventom, A. M., and Bray, R. C. (1995) *Eur. J. Biochem. 232*, 646−657.
28. Leslie, A. G. W. (1992) *Joint CCP4 and ESF-EACMB Newsletter on Protein Crystallography No. 26*, CCLRC, Daresbury Laboratory, Warrington, U.K.
29. Collaborative Computational Project No. 4. (1994) *Acta Crystallogr. D50*, 760−763.
30. Jones, A. T., Zou, J.-Y., Cowan, S. W., and Kjeldgaard, M. (1991) *Acta Crystallogr. A47*, 110−119.
31. Murshudov, G., Vagin, A., and Dodson, E. (1997) *Acta Crystallogr. D53*, 240−255.
32. McEwan, A. G., Wetzstein, H. G., Ferguson, S. J., and Jackson, J. B. (1985) *Biochim. Biophys. Acta 806*, 410−417.
33. Cramer, S. P., Hodgson, K. O., Gillum, W. O., and Mortenson, L. E. (1978) *J. Am. Chem. Soc. 100*, 3398−3407.
34. McNaughton, R. L., Helton, M. E., Rubie, N. D., and Kirk, M. L. (2000) *Inorg. Chem. 39*, 4386−4387.
35. Engman, L., Lind, J., and Merényi, G. (1994) *J. Phys. Chem. 98*, 3174−3182.
36. Heffron, K., Léger, C., Rothery, R. A., Weiner, J. H., and Armstrong, F. A. (2001) *Biochemistry 40*, 3117−3126.
37. Stein, C. A., and Taube, H. (1979) *Inorg. Chem. 18*, 1168−1169.
38. Wagner, M. A., Trickey, P., Chen, Z. W., Mathews, F. S., and Jorns, M. S. (2000) *Biochemistry 39*, 8813−8824.
39. Lim, B. S., Sung, K.-M., and Holm, R. H. (2000) *J. Am. Chem. Soc. 122*, 7410−7411.
40. Buc, J., Santini, C. L., Giordani, R., Czjzek, M., Wu, L. F., and Giordano, G. (1999) *Mol. Microbiol. 32*, 159−168.
41. Weiner, J. H., Rothery, R. A., Sambasivarao, D., and Trieber, C. A. (1992) *Biochim. Biophys. Acta 1102*, 1−18.
42. Smith, A. T., Bray, R. C., McEwan, A. G., McAlpine, A. S., and Bailey, S. (1998) *Biochem Soc. Trans. 26*, S211.
43. Hanlon, S. P., Toh, T.-H., Solomon, P. S., Holt, R. A., and McEwan, A. G. (1996*) Eur. J. Biochem. 239*, 391−396.

BI010559R